Close Approximation of Kullback–Leibler Divergence for Sparse Source Retrieval

Emna Ghodhbani, Mounir Kaaniche, Amel Benazza-Benyahia

Close Approximation of Kullback-Leibler Divergence for Sparse Source Retrieval

Emna Ghodhbani, Mounir Kaaniche, *Member, IEEE* and Amel Benazza-Benyahia

***Abstract*—In this paper, we propose a fast and accurate approximation of the Kullback-Leibler divergence (KLD) between two Bernoulli-Generalized Gaussian (Ber-GG) distributions. Such distribution has been found to be well-suited for modeling sparse signals like wavelet-based representations. Based on high bitrate approximations of the entropy of quantized Ber-GG sources, we provide a close approximation of the KLD without resorting to the conventional time-consuming Monte Carlo estimation approach. The developed approximation formula is then validated in the context of depth map and stereo image retrieval.**

***Index Terms*—Sparse representation, Bernoulli-Generalized Gaussian distribution, Kullback-Leibler divergence, depth maps, stereo image, retrieval.**

I. Introduction

The Kullback-Leibler divergence (KLD) is one of the most fundamental similarity measures in information theory and statistics since it allows to quantify the difference between two statistical models [1]. For this reason, it has been extensively used in various application fields such as image classification and retrieval [2], [3]. For instance, in the context of image retrieval, where wavelet-based approaches have attracted a considerable attention [4], [5], the search is performed by firstly modeling appropriately the probability density functions (pdfs) f_1 and f_2 of respectively the query and the candidate images within the database. Then, their corresponding distributions are compared using the KLD defined as:

$$D_{\mathrm{KL}}(f_1||f_2) = \int_{\mathbb{R}} f_1(\xi) \log_2 \left(\frac{f_1(\xi)}{f_2(\xi)} \right) d\xi. \qquad (1)$$

One of the main advantages of using the KLD is that it can be directly computed from the estimated model parameters for a great number of source models. More precisely, explicit expressions of the KLD have been developed for some univariate distributions such as the Gamma [6], the Weibull [7] and the Generalized Gaussian (GG) [8] ones. Also, ready-to-use formulas exist for the bivariate GG [9] as well as for some Gaussian-copula based multivariate distributions [10], [11]. However, for other statistical models, the integral involved in computing the KLD is analytically intractable, and so, there is no closed-form expression of the KLD. To alleviate this lack, different approximation techniques have been developed in the literature. The most common used approach consists in resorting to Monte Carlo (MC) estimation technique to compute the KLD [12], [13]. While this technique could be used with any source model and should lead to accurate estimation of the KLD, it implies a high computation time in practice. For this reason, other approximation techniques have been investigated for specific models. For instance, for hidden Markov models, an upper bound of the KLD is derived in [14], [15]. Moreover, for Gaussian mixture models, lower and upper bounds approximation as well as variational approximation of the KLD are proposed in [3], [16], [17]. Finally, for a finite mixtures of GG distributions, different KLD approximation methods are used [18] where it has been shown that MC method is the most accurate one.

Among the aforementioned distributions, the GG one has received much attention for modeling the wavelet coefficients of texture images. However, for images with flat regions such as depth maps and, more generally for sparse sources like wavelet representations [19], it has been found that the Bernoulli-Generalized Gaussian (Ber-GG) distribution becomes more appropriate for modeling their coefficients [20]. Therefore, in order to provide a more general framework, the objective of this paper is to focus on the computation of the KLD between two Ber-GG models. More precisely, we first derive a close approximation of the KLD based on an accurate estimation of the entropy of quantized Ber-GG sources at high bitrates. This allows us to easily deduce its symmetric version known as the Jeffreys divergence (JD) [21]. It is worth pointing out that the obtained results remain also valid for standard images which are often modeled using GG distribution and, more generally for any sparse source. Our second contribution deals with the benefits of the proposed approximations for the retrieval of depth maps and stereo images.

In Sec. II, we present the main idea behind this work and define the retained source and quantization models. In Sec. III, close approximations of the KLD and JD between two Ber-GG models are provided. Finally, experimental results are shown in Sec. IV, and some conclusions are drawn in Sec. V.

II. Methodology

A. Motivation

The KLD, given by Eq. (1), can be rewritten as:

$$D_{\mathrm{KL}}(f_1 \parallel f_2) = H_{f_1,f_2} - H_{f_1}, \qquad (2)$$

where H_{f_1,f_2} denotes the cross entropy between f_1 and f_2 and H_{f_1} is the entropy of f_1. Given the recent approximation of the entropy of a quantized Ber-GG source with a quantization step q [20], and knowing that at high bitrate, the quantization

E. Ghodhbani and A. Benazza-Benyahia are with the University of Carthage, SUP'COM, LR11TIC01, Communications, Signal and Image (COSIM) Lab., Ariana, 2083. e-mail: {emna.ghodbani,benazza.amel}@supcom.tn.

M. Kaaniche is with Laboratoire de Traitement et Transport de l'Information, Institut Galilée, Université Paris 13, Sorbonne Paris Cité, 93430 Villetaneuse, France. e-mail: mounir.kaaniche@univ-paris13.fr.

error is very small (i.e. the output of the quantizer is very close to the input), we are motivated to estimate the KLD and the JD between two Ber-GG sources X_1 and X_2 based on the approximations of H_{f_1,f_2} and H_{f_1} of the quantized sources at high bitrates. To this end, let us first recall the retained source and quantization models.

B. Source and quantization models

In a typical wavelet-based decomposition, the sources X_1 and X_2 correspond to each two wavelet subbands having the same orientation and the same scale of the multiscale representations of two images. To better capture the sparsity of the resulting wavelet subband coefficients, Bernoulli-based models have been widely used in the literature. For instance, Bernoulli-Gaussian distribution has been successfully applied to select the best wavelet packet representation for 1D signals [22] or to denoise images [23]. Recently, the Ber-GG model has been found to be more general and appropriate for sparse source coding [20] and sparse signal recovery [24]. For this reason, we assume here that the source coefficients are modeled using the Ber-GG distribution whose pdf is given by:

$$\begin{aligned}&\forall \mathrm{k} \in \{1,2\},\ \forall \xi \in \mathbb{R},\\ &\quad f_{\mathrm{k}}(\xi;\epsilon_{\mathrm{k}},\omega_{\mathrm{k}},\beta_{\mathrm{k}}) = (1-\epsilon_{\mathrm{k}})\delta(\xi) + \epsilon_{\mathrm{k}}\widetilde{f}_{\mathrm{k}}(\xi;\omega_{\mathrm{k}},\beta_{\mathrm{k}}),\end{aligned} \tag{3}$$

where $\epsilon_{\mathrm{k}} \in [0,1]$ represents the mixture parameter, δ denotes the Dirac distribution, and $\widetilde{f}_{\mathrm{k}}$ is the pdf of the GG distribution:

$$\forall \xi \in \mathbb{R}, \widetilde{f}_{\mathrm{k}}(\xi;\omega_{\mathrm{k}},\beta_{\mathrm{k}}) = \frac{\beta_{\mathrm{k}}\omega_{\mathrm{k}}^{1/\beta_{\mathrm{k}}}}{2\Gamma(1/\beta_{\mathrm{k}})}\exp^{-\omega_{\mathrm{k}}|\xi|^{\beta_{\mathrm{k}}}} \tag{4}$$

$\Gamma(\cdot)$ being the Gamma function and, ω_{k} and β_{k} are the scale and shape parameters that can be estimated using the maximum likelihood criterion [8].

Moreover, we assume that each subband coefficient is quantized using a uniform scalar quantizer with a quantization step q and a deadzone of size $(2\tau-1)q$ where $\tau > \frac{1}{2}$ [25]. For each input source $X_{\mathrm{k}} = \left(x_{\mathrm{k},s}\right)$ where $\mathrm{k} \in \{1,2\}$ and s represents the source coefficient index, the output of the quantizer $\overline{X}_{\mathrm{k}} = \left(\overline{x}_{\mathrm{k},s}\right)$ can be expressed as:

$$\overline{x}_{\mathrm{k},s} = r_0 = 0, \qquad \text{if } |x_{\mathrm{k},s}| < \left(\tau - \tfrac{1}{2}\right)q, \quad \text{where } \tau > 1/2$$

and, for all $i \in \mathbb{Z}$, $\overline{x}_{\mathrm{k},s} = r_{\mathrm{k},i}$,

$$\begin{aligned}&(\text{if } (\tau+i-\tfrac{3}{2})q \le x_{\mathrm{k},s} < (\tau+i-\tfrac{1}{2})q \text{ and } i \ge 1)\\ &\text{or } (\text{if } (-\tau+i+\tfrac{1}{2})q < x_{\mathrm{k},s} \le (-\tau+i+\tfrac{3}{2})q \text{ and } i \le -1),\end{aligned}$$

where $r_{\mathrm{k},i}$ denotes the reconstruction levels given by

$$\forall i \ge 1, \qquad r_{\mathrm{k},i} = -r_{\mathrm{k},-i} = (\tau+i-1)q. \tag{5}$$

Note that this quantizer corresponds to the standard scheme used in conventional wavelet-based coding methods [26].

III. KLD and JD between two Bernoulli-GG distributions

In order to provide approximations of the KLD and JD between two Ber-GG sources, we will focus on the entropy H_{f_1} and cross-entropy H_{f_1,f_2} of their quantized versions.

A. Entropy and cross-entropy approximations

According to recent approximations of rate-distortion functions developed in [20], it has been shown that at high bitrate, the entropy H_{f_1} of a Ber-GG source can be written as:

$$H_{f_1} = \widehat{H}_{f_1}(q) + o(q\log_2 q) \tag{6}$$

where $\widehat{H}_{f_1}$ is the high rate approximation of the entropy:

$$\widehat{H}_{f_1}(q) = H_{\epsilon_1} + \epsilon_1(h_{\beta_1}(\omega_1) - \log_2 q), \tag{7}$$

with H_{ϵ_1} is the entropy of a Bernoulli variable of parameters $(1-\epsilon_1,\epsilon_1)$:

$$H_{\epsilon_1} = -\epsilon_1\log_2\epsilon_1 - (1-\epsilon_1)\log_2(1-\epsilon_1), \tag{8}$$

and $h_{\beta_1}(\omega_1)$ is the differential entropy of the GG variable of parameters (β_1,ω_1):

$$h_{\beta_1}(\omega_1) = \log_2\Big(\frac{2\Gamma(1/\beta_1)}{\beta_1\omega_1^{1/\beta_1}}\Big) + \frac{1}{\beta_1}. \tag{9}$$

Regarding the second term H_{f_1,f_2}, let us recall that the cross-entropy of the quantized signals is defined by:

$$\begin{aligned}H_{f_1,f_2} &= -\sum_{i=-\infty}^{\infty}\mathsf{p}_{1,i}\log_2\mathsf{p}_{2,i}\\ &= -\mathsf{p}_{1,0}\log_2\mathsf{p}_{2,0} - 2\sum_{i=1}^{\infty}\mathsf{p}_{1,i}\log_2\mathsf{p}_{2,i}\end{aligned} \tag{10}$$

where, for each $\mathrm{k} \in \{1,2\}$, $\mathsf{p}_{k,i} = \mathsf{P}(\overline{x}_{k,s} = r_{k,i})$ is the probability of occurrence of the reconstruction level $r_{\mathrm{k},i}$. It can be checked that the probability of the zero and i-th ($i \ge 1$) reconstruction levels $r_{k,i}$ can be expressed as follows:

$$\begin{cases}\mathsf{p}_{\mathrm{k},0} &= (1-\epsilon_{\mathrm{k}}) + \epsilon_{\mathrm{k}}\widetilde{\mathsf{p}}_{\mathrm{k},0}\\ \mathsf{p}_{\mathrm{k},i} &= \epsilon_{\mathrm{k}}\widetilde{\mathsf{p}}_{\mathrm{k},i}, \qquad \forall i \ge 1.\end{cases} \tag{11}$$

where

$$\widetilde{\mathsf{p}}_{\mathrm{k},0} = 2\int_0^{q(\tau-\frac{1}{2})}\widetilde{f}_{\mathrm{k}}(\xi)d\xi = Q_{1/\beta_{\mathrm{k}}}\Big(\omega_{\mathrm{k}}\big((\tau-\frac{1}{2})q\big)^{\beta_{\mathrm{k}}}\Big) \tag{12}$$

and, for $i \ge 1$,

$$\begin{aligned}\widetilde{\mathsf{p}}_{\mathrm{k},i} = \int_{(\tau+i-\frac{3}{2})q}^{(\tau+i-\frac{1}{2})q}\widetilde{f}_{\mathrm{k}}(\xi)d\xi &= \frac{1}{2}\Big(Q_{1/\beta_{\mathrm{k}}}\Big(\omega_{\mathrm{k}}\big((\tau+i-\frac{1}{2})q\big)^{\beta_{\mathrm{k}}}\Big)\\ &\quad - Q_{1/\beta_{\mathrm{k}}}\Big(\omega_{\mathrm{k}}\big((\tau+i-\frac{3}{2})q\big)^{\beta_{\mathrm{k}}}\Big)\Big).\end{aligned} \tag{13}$$

with $Q_{1/\beta_{\mathrm{k}}}$ is the normalized incomplete Gamma function. Thus, the cross-entropy H_{f_1,f_2}, given by Eq. (10), becomes

$$\begin{aligned}H_{f_1,f_2} &= -(1-\epsilon_1+\epsilon_1\widetilde{\mathsf{p}}_{1,0})\log_2(1-\epsilon_2+\epsilon_2\widetilde{\mathsf{p}}_{2,0})\\ &\quad - 2\epsilon_1\left(\sum_{i=1}^{\infty}\widetilde{\mathsf{p}}_{1,i}\log_2\widetilde{\mathsf{p}}_{2,i} + \log_2\epsilon_2\sum_{i=1}^{\infty}\widetilde{\mathsf{p}}_{1,i}\right)\\ &= -(1-\epsilon_1+\epsilon_1\widetilde{\mathsf{p}}_{1,0})\log_2(1-\epsilon_2+\epsilon_2\widetilde{\mathsf{p}}_{2,0})\\ &\quad + \epsilon_1\left(H_{\widetilde{f}_1,\widetilde{f}_2} + \widetilde{\mathsf{p}}_{1,0}\log_2\widetilde{\mathsf{p}}_{2,0}\right)\\ &\quad - (1-\widetilde{\mathsf{p}}_{1,0})\epsilon_1\log_2\epsilon_2.\end{aligned} \tag{14}$$

where $H_{\widetilde{f}_1,\widetilde{f}_2}$ is the cross-entropy between the two GG variables $\widetilde{f}_1$ and $\widetilde{f}_2$.

By noticing that $H_{\widetilde{f}_1,\widetilde{f}_2}$ can also be expressed with respect to

the KLD between $\widetilde{f}_1$ and $\widetilde{f}_2$, which has already a closed-form expression, Eq. (14) can be rewritten as:

$$\begin{aligned} H_{f_1,f_2} &= -(1-\epsilon_1+\epsilon_1\widetilde{\mathsf{p}}_{1,0})\log_2(1-\epsilon_2+\epsilon_2\widetilde{\mathsf{p}}_{2,0}) \\ &+ \epsilon_1\Big(D_{\mathrm{KL}}(\widetilde{f}_1 \parallel \widetilde{f}_2) + H_{\widetilde{f}_1} + \widetilde{\mathsf{p}}_{1,0}\log_2\widetilde{\mathsf{p}}_{2,0}\Big) \\ &- (1-\widetilde{\mathsf{p}}_{1,0})\epsilon_1\log_2\epsilon_2. \end{aligned} \tag{15}$$

Let us now focus on the approximation of this cross-entropy term at high bitrate. In this case (i.e. when $q \to 0$), the entropy $H_{\widetilde{f}_1}$ of a GG variable is given by

$$H_{\widetilde{f}_1}(q) = \widehat{H}_{\widetilde{f}_1}(q) + o(q), \tag{16}$$

where

$$\widehat{H}_{\widetilde{f}_1}(q) = h_{\beta_1}(\omega_1) - \log_2 q \tag{17}$$

Moreover, for all $a > 0$ [27], $Q_a(\xi) = o(\xi^a) \quad \text{as} \quad \xi \to 0$:

$$\widetilde{\mathsf{p}}_{k,0} = Q_{1/\beta_k}\Big(\omega_k\big((\tau-\frac{1}{2})q\big)^{\beta_k}\Big) = o(q). \tag{18}$$

Therefore, H_{f_1,f_2} reads to:

$$H_{f_1,f_2} = \widehat{H}_{f_1,f_2}(q) + o(q) \tag{19}$$

with:

$$\begin{aligned} \widehat{H}_{f_1,f_2}(q) &= -(1-\epsilon_1)\log_2(1-\epsilon_2) - \epsilon_1\log_2\epsilon_2 \\ &+ \epsilon_1\Big(D_{\mathrm{KL}}(\widetilde{f}_1 \parallel \widetilde{f}_2) + h_{\beta_1}(\omega_1) - \log_2 q\Big). \end{aligned} \tag{20}$$

B. KLD and JD formulas

By combining Eqs. (2), (6), (7), (8), (19) and (20), a closed-form approximation of the KLD can be obtained as follows:

$$\begin{aligned} \widehat{D}_{\mathrm{KL}}(f_1 \parallel f_2) =& \epsilon_1 D_{\mathrm{KL}}(\widetilde{f}_1 \parallel \widetilde{f}_2) + \epsilon_1\log_2\left(\frac{\epsilon_1}{\epsilon_2}\right) \\ &+ (1-\epsilon_1)\log_2\left(\frac{1-\epsilon_1}{1-\epsilon_2}\right) \end{aligned} \tag{21}$$

where $D_{\mathrm{KL}}(\widetilde{f}_1 \parallel \widetilde{f}_2)$ is the KLD between the two GG variables given by [8]:

$$\begin{aligned} D_{\mathrm{KL}}(\widetilde{f}_1 \parallel \widetilde{f}_2) =& \log\Big(\frac{\beta_1\omega_1^{1/\beta_1}\Gamma(1/\beta_2)}{\beta_2\omega_2^{1/\beta_2}\Gamma(1/\beta_1)}\Big) - \frac{1}{\beta_1} \\ &+ \Big(\frac{\omega_2^{1/\beta_2}}{\omega_1^{1/\beta_1}}\Big)^{\beta_2}\frac{\Gamma((\beta_2+1)/\beta_1)}{\Gamma(1/\beta_1)}. \end{aligned} \tag{22}$$

Furthermore, one should note that it is often required to employ symmetric distances in various application fields, such as the retrieval. As a result, we also propose to consider the JD which is defined as:

$$JD(f_1 \parallel f_2) = D_{\mathrm{KL}}(f_1 \parallel f_2) + D_{\mathrm{KL}}(f_2 \parallel f_1). \tag{23}$$

Consequently, thanks to Eq. (21), it can be deduced that the JD between two Ber-GG distributions can be approximated and computed as follows:

$$\begin{aligned} \widehat{JD}(f_1 \parallel f_2) &= \epsilon_1 D_{\mathrm{KL}}(\widetilde{f}_1 \parallel \widetilde{f}_2) + \epsilon_2 D_{\mathrm{KL}}(\widetilde{f}_2 \parallel \widetilde{f}_1) \\ &+ (\epsilon_1-\epsilon_2)\log_2\left(\frac{\epsilon_1}{\epsilon_2}\right) + (\epsilon_2-\epsilon_1)\log_2\left(\frac{1-\epsilon_1}{1-\epsilon_2}\right). \end{aligned} \tag{24}$$

C. Discussions

Some comments can be made about the obtained KLD and JD formulas. First, contrary to high bitrate approximation of the entropy and cross-entropy functions, which are expressed with respect to the quantization step q, it is interesting to note that the obtained approximations of the KLD and the JD in Eqs. (21) and (24) are independent of q. Thus, the KLD and JD can be directly computed without performing the quantization of the sources and knowing only the estimated statistical parameters $(\epsilon_k, \omega_k, \beta_k)$ of the two Ber-GG models. Moreover, when $\epsilon_1 = \epsilon_2 = 1$ (i.e. the input sources follow a GG distribution), it can be checked that Eq. (21) (resp. Eq. (24)) leads to the well-known KLD (resp. JD) expression between two GG variables. Therefore, the developed formulas remain also valid for comparing GG distributions.
Finally, when $\epsilon_1 \simeq \epsilon_2 = \epsilon$, the computation of KLD and JD between two Ber-GG sources will be simply reduced to the computation of these divergences between their respective GG distributions. In this case, we have

$$\begin{cases} \widehat{D}_{\mathrm{KL}}(f_1 \parallel f_2) &= \epsilon D_{\mathrm{KL}}(\widetilde{f}_1 \parallel \widetilde{f}_2) \\ \widehat{JD}(f_1 \parallel f_2) &= \epsilon JD(\widetilde{f}_1 \parallel \widetilde{f}_2). \end{cases} \tag{25}$$

IV. Application to depth maps and stereo images retrieval

The developed KLD and JD can be useful for comparing sparse sources in the context of transform-based retrieval application. For this reason, we propose to validate our approximations by focusing on depth maps which represent the 3D information of a given scene. To this respect, we used the standard Tsukuba stereo images (SI) dataset [28] which consists of $1,800$ stereo scenes as well as their associated ground truth depth maps, of size 640×480. Although this database was previously used in other stereo vision applications [29], [30], it has been adapted to be exploited in the retrieval context. To this end, each dataset is divided into 17 classes according to their visual contents. Moreover, Daubechies wavelets of order 8 are chosen for the multiscale decomposition of the SI and the depth maps, over three resolution levels. At the indexing step, the statistical parameters are first extracted from the detail subbands of the query and candidate database images. Then, these parameters, considered as salient features, are compared using the symmetric KLD (i.e. JD). While the KLD has been developed in Sections II and III for a given two wavelet subbands, it should be noted that the global similarity measure between two images is obtained by taking the sum of the KLD of all the detail wavelet subbands of both images.
Let us first study the accuracy of the retained Ber-GG distribution for modeling the wavelet coefficients of the depth maps. As mentioned in Section I, Bernoulli-based distributions have been recently used for different sparse signal problems. For this reason and, in addition to the widely used GG model, we have considered the Bernoulli-Gaussian as well as the Bernoulli-Laplacian models. The accuracy of these models is evaluated using the Kolmogorov Smirnov (KS) test. More precisely, Table I provides the average KS values obtained with the detail subbands of the whole depth maps dataset.

Thus, it can be firstly noticed that the standard GG model leads to lower KS value compared to the Bernoulli-Gaussian and Laplacian models. Most importantly, the obtained results show that the Ber-GG model yields the smallest KS value which corroborates its appropriateness for modeling sparse representations. For instance, from Fig. 1 illustrating the histogram of the wavelet coefficients of a given detail subband as well as their modeling step using the different distributions, one can confirm again that the Ber-GG model is more accurate than the other ones for modeling sparse coefficients.

TABLE I
AVERAGE KS VALUES OBTAINED WITH DIFFERENT STATISTICAL MODELING OF THE DETAIL SUBBANDS OF THE DEPTH MAPS DATASET.

Model	Ber-Laplacian	Ber-Gaussian	GG	Ber-GG
KS	0.34	0.33	0.25	**0.08**

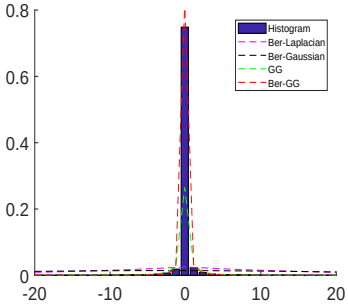

Fig. 1. Histogram of a vertical detail subband and its statistical modeling using different distributions.

To show the relevance of the proposed approximation results, two rounds of experiments have been carried out. The first one is devoted to the indexing of the depth maps dataset. Since the GG model has been found to be more accurate than the Bernoulli-Gaussian and Laplacian models as shown in Table I, we will consider the standard GG model (approach denoted by "D-GG") and the retained Ber-GG one to extract the statistical features from the depth maps. For the latter model, and in order to compute the KLD between the distributions of the query and database depth maps, we used the well-known MC estimation approach as well as the proposed analytic expression, which will be respectively designated by "D-Ber.GG-MC" and "D-Ber.GG-Analytic". Let us recall that the MC approximation of the KLD between f_1 and f_2 consists first in iteratively generating a set of random sample data $(x_1, x_2, \ldots, x_n)$ based on the model density f_1. Then, the KLD can be estimated by:

$$\tilde{D}_{\mathrm{KL}}(f_1 \parallel f_2) \simeq \frac{1}{n}\sum_{i=1}^{n} \log_2 f_1(x_i) - \log_2 f_2(x_i). \qquad (26)$$

Fig. 2(a) shows the Precision (PR)-Recall (RC) performance of the different retrieval approaches. First, it can be observed that the Ber-GG-based depth map modeling approach outperforms the conventional GG-based modeling technique. Moreover, the standard MC method as well as the proposed analytic one result in similar retrieval performances, which confirms the accuracy of our theoretical results. It is important to note here that the main advantage of the proposed approximation is that it allows a fast computation of the KLD contrary to the time consuming MC approach. Indeed, using a computer with an Intel Core i7 processor (2.6 GHz) and a Matlab implementation, the computation of the KLD between two images of the dataset takes 1.25 (resp. 0.001) seconds with the standard MC (resp. proposed analytic) approach.

Since the indexing of the depth maps has been found to be very interesting in the context of SI retrieval [31], [32], the second round of our experiments has been devoted to the retrieval of the "Flashlight" Tsukuba SI dataset. More precisely, four retrieval approaches are considered. In the first one, only statistical parameters of the detail subbands of the query and candidates SI are used as texture features. Since the GG distribution is well known to be appropriate for modeling the wavelet coefficients of texture and natural images, the statistical features of the left and right views are extracted using the univariate GG modeling approach [31]. This approach will be designated by "LR-GG". The remaining three approaches, combine the texture features with the depth ones which are obtained by following the methods considered in the first round of our experiments. Therefore, these three approaches will be denoted by "LR-GG-D-GG", "LR-GG-D-Ber. GG-MC" and "LR-GG-D-Ber. GG-Analytic". It should be noted here that the global similarity measure between two SIs is obtained by computing the sum of the three KLD values obtained with the left view, the right one and, the depth map. The PR-RC curves are illustrated in Fig. 2(b) and show that the "LR-GG-D-GG" approach leads to a substantial gain compared to the "LR-GG" one. This clearly outlines the benefits of exploiting the depth maps in SI retrieval application. Moreover, further improvements are achieved by modeling the depth maps with a Ber-GG distribution. Finally, it can be also observed that our KLD approximation yields similar performance compared to the MC approach.

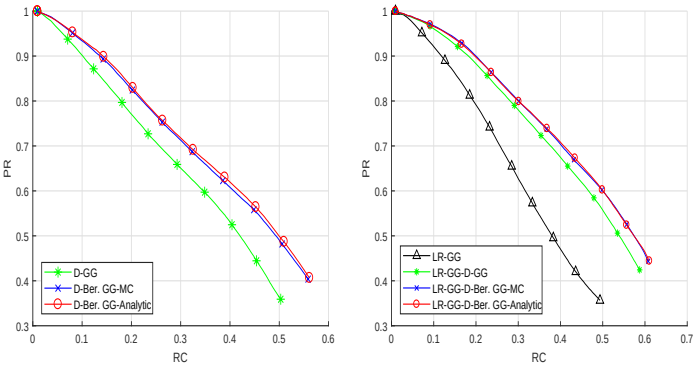

Fig. 2. Precision-Recall curves of the: (left side) depth maps retrieval process, (right side) depth-based stereo images retrieval process.

V. CONCLUSION

In this paper, we proposed accurate and ready-to-use approximations of the KLD and JD between two sparse Bernoulli Generalized Gaussian sources. The proposed approximations depend only on the estimated distribution parameters and present the advantage of allowing fast computation of these divergences. The benefits of the developed formulas have been shown in the context of depth maps and wavelet-based stereo image retrieval.

REFERENCES

[1] S. Kullback and R. A. Leibler, "On information and sufficiency," *Annals of Mathematical Statistics*, vol. 22, no. 1, pp. 79–86, 1951.

[2] X. Qin, H. Zou, S. Zhou, and K. Ji, "Region-based classification of SAR images using Kullback-Leibler distance between generalized gamma distributions," *IEEE Geoscience and Remote Sensing Letters*, vol. 12, no. 8, pp. 1655–1659, 2015.

[3] S. Cui, "Comparison of approximation methods to Kullback-Leibler divergence between Gaussian mixture models for satellite image retrieval," *Remote Sensing Letters*, vol. 7, no. 7, pp. 651–660, 2016.

[4] E. de Ves, A. Ruedin, D. Acevedo, X. Benavent, and L. Seijas, "A new wavelet-based texture descriptor for image retrieval," in *International Conference on Computer Analysis of Images and Patterns*, 2007, pp. 895–902.

[5] R. Kwitt and A. Uhl, "Lightweight probabilistic texture retrieval," *IEEE Transactions on Image Processing*, vol. 19, no. 1, pp. 241–253, 2010.

[6] J. R. Mathiassen, A. Skavhaug, and K. Bø, "Texture similarity measure using Kullback-Leibler divergence between gamma distributions," in *European Conference on Computer Vision*. Springer, 2002, pp. 133–147.

[7] R. Kwitt and A. Uhl, "Image similarity measurement by Kullback-Leibler divergences between complex wavelet subband statistics for texture retrieval," in *International Conference on Image Processing*, 2008, pp. 933–936.

[8] M. N. Do and M. Vetterli, "Wavelet-based texture retrieval using generalized Gaussian density and Kullback-Leibler distance," *IEEE Transactions on Image Processing*, vol. 11, no. 2, pp. 146–158, 2002.

[9] G. Verdoolaege, Y. Rosseel, M. Lambrechts, and P. Scheunders, "Wavelet-based colour texture retrieval using the Kullback-Leibler divergence between bivariate generalized gaussian models," in *International Conference on Image Processing*, 2009, pp. 265–268.

[10] N.-E. Lasmar and Y. Berthoumieu, "Gaussian copula multivariate modeling for texture image retrieval using wavelet transforms," *IEEE Transactions on Image Processing*, vol. 23, no. 5, pp. 2246–2261, 2014.

[11] C. Li, G. Duan, and F. Zhong, "Rotation invariant texture retrieval considering the scale dependence of Gabor wavelet," *IEEE Transactions on Image Processing*, vol. 24, no. 8, pp. 2344–2354, 2015.

[12] R. Kwitt and A. Uhl, "A joint model of complex wavelet coefficients for texture retrieval," in *International Conference on Image Processing*, 2009, pp. 1877–1880.

[13] S. Sakji-Nsibi and A. Benazza-Benyahia, "Fast scalable retrieval of multispectral images with Kullback–Leibler divergence," in *International Conference on Image Processing*, 2010, pp. 2333–2336.

[14] M. N. Do and M. Vetterli, "Rotation invariant texture characterization and retrieval using steerable wavelet-domain hidden Markov models," *IEEE Transactions on Multimedia*, vol. 4, no. 4, pp. 517–527, 2002.

[15] J. Silva and S. Narayanan, "Upper bound Kullback–Leibler divergence for transient hidden Markov models," *IEEE Transactions on Signal Processing*, vol. 56, no. 9, pp. 4176–4188, 2008.

[16] J.-L. Durrieu, J.-P. Thiran, and F. Kelly, "Lower and upper bounds for approximation of the Kullback-Leilbler divergence between Gaussian mixture models," in *International Conference on Acoustics Speech and Signal Processing*, 2012, p. 4 pages.

[17] F. Nielsen and K. Sun, "Guaranteed bounds on the Kullback–Leibler divergence of univariate mixtures," *IEEE Signal Processing Letters*, vol. 23, no. 11, pp. 1543–1546, 2016.

[18] M. S. Allili, "Wavelet modeling using finite mixtures of generalized gaussian distributions: application to texture discrimination and retrieval." *IEEE Trans. Image Processing*, vol. 21, no. 4, pp. 1452–1464, 2012.

[19] S. Mallat, *A Wavelet Tour of Signal Processing: The Sparse Way*, 3rd ed. Orlando, FL, USA: Academic Press, Inc., 2008.

[20] M. Kaaniche, A. Fraysse, B. Pesquet-Popescu, and J.-C. Pesquet, "A bit allocation method for sparse source coding," *IEEE Transactions on Image Processing*, vol. 23, no. 1, pp. 137–152, 2014.

[21] H. Jeffreys, "An invariant form for the prior probability in estimation problems," in *Proceedings of the Royal Society of London. Series A. Mathematical and Physical Sciences*, 1946, pp. 453–461.

[22] J.-C. Pesquet, H. Krim, D. Leporini, and E. Hamman, "Bayesian approach for best basis selection," in *IEEE International Conference on Acoustics, Speech and Signal Processing*, Atlanta, USA, May 1996, pp. 2634–2638.

[23] A. Benazza-Benyahia, J. C. Pesquet, and C. Chaux, "Building robust wavelet estimators for multicomponent images using Steins principle," *IEEE Transactions on Image Processing*, vol. 14, pp. 1814–1830, 2005.

[24] L. Chaari, J.-Y. Toumeret, and C. Chaux, "Sparse signal recovery using a Bernoulli generalized Gaussian prior," in *European Signal Processing Conference*, 2015, pp. 1711–1715.

[25] A. Gersho and R. Gray, *Vector Quantization and Signal Compression*. Boston, MA: Kluwer, 1992.

[26] D. Taubman, "High performance scalable image compression with EBCOT," *IEEE Transactions on Image Processing*, vol. 9, no. 7, pp. 1158–1170, 2000.

[27] L. S. Gradshteyn and L. M. Ryzhik, *Tables of Integrals, Series and Products*. San Diego: Academic press, 2000.

[28] S. Martull, M. Peris, and K. Fukui, "Realistic CG stereo image dataset with ground truth disparity maps," in *International Conference on Pattern Recognition, Workshop TrakMark2012*, 2012, pp. 40–42.

[29] G. Riegler, M. Rüther, and H. Bischof, "ATGV-Net: Accurate depth super-resolution," in *European Conference on Computer Vision*. Springer, 2016, pp. 268–284.

[30] A. Patron-Perez, S. Lovegrove, and G. Sibley, "A spline-based trajectory representation for sensor fusion and rolling shutter cameras," *International Journal of Computer Vision*, vol. 113, no. 3, pp. 208–219, 2015.

[31] A. Chaker, M. Kaaniche, and A. Benazza-Benyahia, "Disparity based stereo image retrieval through univariate and bivariate models," *Signal Processing: Image Communication*, vol. 31, pp. 174–184, 2015.

[32] A. Karine, A. D. El Maliani, and M. El Hassouni, "A novel statistical model for content-based stereo image retrieval in the complex wavelet domain," *Journal of Visual Communication and Image Representation*, vol. 50, pp. 27–39, 2018.